Journal of Chromatography A, 1218 (2011) 3966–3972

Contents lists available at ScienceDirect

Journal of Chromatography A

journal homepage: www.elsevier.com/locate/chroma

Influence of protein adsorption kinetics on breakthrough broadening in membrane affinity chromatography

Simone Dimartino[1], Cristiana Boi, Giulio C. Sarti*

Dipartimento di Ingegneria Chimica, Mineraria e delle Tecnologie Ambientali, DICMA, Alma Mater Studiorum-Università di Bologna, via Terracini 28, 40131 Bologna, Italy

ARTICLE INFO

Article history:
Received 11 February 2011
Received in revised form 24 March 2011
Accepted 21 April 2011
Available online 6 May 2011

Keywords:
Affinity membranes
Adsorption kinetics
Immunoglobulin G
Breakthrough
Model simulations
Bi-Langmuir isotherm

ABSTRACT

Existing mathematical models developed to describe membrane affinity chromatography are unable to match the complete breakthrough curve when a single Langmuir adsorption isotherm is used, because important deviations from the observed behavior are systematically encountered in the simulation of breakthrough broadening near saturation. The relevant information required to overcome that limitation has been obtained by considering simultaneously both loading and washing curves, thus evaluating the adsorption data at equilibrium and recognizing what are the appropriate adsorption mechanisms affecting the observed behavior. The analysis indicates that a bi-Langmuir binding kinetics is essential for a correct process description up to the saturation of the stationary phase, together with the use of the relevant transport phenomena already identified for the experimental system investigated. The input parameters used to generate the resulting simulations are evaluated from separate experiments, independent from the chromatographic process. Model calibration and validation is accomplished comparing model simulations with experimental data measured by feeding pure human immunoglobulin G (IgG) solutions as well as a cell culture supernatant containing human monoclonal IgG_1 to B14-TRZ-Epoxy2 bio-mimetic affinity membranes. The simulations obtained are in good agreement with the experimental data over the entire adsorption and washing stages, and breakthrough tailing appears to be associated to the reversible binding sites of the bi-Langmuir mechanism. Remarkably, the model proposed is able to predict with good accuracy the purification of IgG from a complex mixture simply on the basis of the results obtained from pure IgG solutions.

1. Introduction

Therapeutic antibodies manufacture is a key issue in the biotechnology industry, and their production at a large scale has become increasingly important with the recent approval of several drugs of this class for different critical illnesses [1,2]. Downstream processing is recognized as the bottleneck in current antibody production platforms [3,4] and its optimization is a prerequisite for important reductions of antibodies production costs.

At present, antibody capture with Protein A resins is the most expensive step among the unit operations involved in downstream processing, which can contribute up to 50–80% of the total purification costs [5]. However, a huge optimization potential is expected [6] as a result of the increasing efforts devoted to the development of possible alternatives to the canonical bead based Protein A affinity chromatography.

Mimetic affinity membrane chromatography is particularly attractive to that aim, because it combines the advantages of mimetic ligands, in terms of antibody specificity and lower manufacture costs [7–9], with membrane technology, which introduces its superior mass transport characteristics, high throughput and absence of pressure drop issues [10–13]. In order to pursue an industrial application of that technique, an effective modeling tool is needed to predict reliably the process performance also in large-scale modules, as required for scale-up design and optimization purposes.

The modeling and simulation of an affinity chromatographic cycle has been considered in several works. The basic approach is the combination of a species mass balance equation coupled with a kinetic equation to represent the protein adsorption/desorption mechanism on the surface active sites [14,15]. The binding kinetics generally adopted to describe the protein–ligand interaction is represented by a simple reversible Langmuir model [16,17], even though that is unable to reproduce the complete experimental breakthrough, especially near membrane saturation where a typical broadening is frequently observed [18–20].

Different binding kinetics have been proposed in the literature in order to accurately describe breakthrough broadening close to

* Corresponding author. Tel.: +39 051 2090251; fax: +39 051 2090247.
E-mail address: giulio.sarti@unibo.it (G.C. Sarti).
[1] Present address: Biomolecular Interaction Centre (BIC), University of Canterbury, Christchurch, New Zealand.

0021-9673/$ – see front matter © 2011 Elsevier B.V. All rights reserved.
doi:10.1016/j.chroma.2011.04.062

saturation conditions: Shi et al. proposed a kinetic equation based on Freundlich model [21], while Yang and Etzel considered the possibility of a steric hindrance resistance at high surface coverages, as well as the conformational changes that a protein may experience when bound to a surface [22]. The simulation results presented in those works are fairly adequate to approximate the onset of the experimental breakthrough curves, but the simulations still do not match the tailing behavior close to membrane saturation. The goal to represent well the entire breakthrough curve up to saturation might be considered an unnecessary refinement since in actual practice breakthrough point is well below complete column saturation and usually does not exceed 10% of feed concentration. However, the initial layers of the stationary phase, encountered close to feed entrance, may have already reached their saturation while subsequent layers still remain with little loading. Thus, a better understanding of the membrane behavior up to saturation appears indeed important also for the actual chromatography practice.

Based on the analysis of both adsorption and washing stages, in the present work the origin of breakthrough broadening is ascribed to the co-existence of two different and independent binding sites, with two different binding kinetics, which leads to a bi-Langmuir adsorption mechanism. This heterogeneous binding kinetics is similar to the one used by Wang and Carbonell for staphylococcal enterotoxin B adsorption onto a bio-mimetic affinity resin [23] and by Boi et al. for IgG adsorption on mimetic A2P affinity membranes [24]. The above binding kinetics is used in the general simulation model for membrane chromatography which has been described in detail in a recent work [25], obtaining simulations suitable to describe the entire chromatographic cycle, including the behavior observed in breakthrough curves close to saturation. Interestingly, the resulting complete model presented in this work is characterized by two main advantages in comparison to the previous version based on a single (reversible or irreversible) Langmuir model: (i) it is not limited to describe breakthrough curves up to 80% saturation (which still is an appreciable result), and consequently does not require to estimate the proper reduction of the maximum binding capacity of the membrane, as discussed in Ref. [25] for the previous model; (ii) in addition, use of the bi-Langmuir kinetics allows to overcome conceptual inconsistency of the previous models where a reversible Langmuir kinetics was used during adsorption stage, while no reaction was considered during washing, even if no buffer changes were introduced in the washing stage.

The experimental reference system considered for model validation is the purification of human IgG through mimetic B14-TRZ-Epoxy2 membranes, which have been produced and studied in view of the actual interest on mimetic ligands [26]. This material consists of a highly interconnected porous matrix, where mimetic ligand B14 is immobilized onto the pore surface through a triazole ring (TRZ) spacer. These new affinity membranes combine the highly accessible internal structure of Epoxy2 membranes with the benefits of B14 ligand, represented by high specificity towards IgG and pluronic F68 tolerance. In addition, an industrial application of this chromatographic medium results particularly promising as significant improvements in its binding capacity are expected [26].

Main contributions of the present work are represented by the use of a proper adsorption kinetic expression, obtained from simultaneous analysis of experimental observations during loading and washing stages. That leads (a) to a rather satisfactory model simulations of the chromatographic cycles up to complete membrane saturation, and (b) to a rather satisfactory description of the washing stage, with no need to artificially change binding/unbinding kinetics in this stage, in absence of changes in the buffer used. In fact, the washing stage is often disregarded because of its minor importance in process practice, but its accurate analysis was found very useful as many important information on binding kinetics and thermodynamics can be extracted from the washing profile.

2. Experimental

The equipment and materials used in the experiments performed are the same as those reported in Refs. [25] and [26]; for clarity sake the experimental set up and procedures adopted to evaluate numerical values of model parameters are briefly recalled in the following.

The experimental system considers the purification of human IgG_1 from a cell culture supernatant by using B14-TRZ-Epoxy2 affinity membranes. A layered stack of 5 membranes with total thickness of 0.1 cm and a diameter of 2.5 cm, was allocated into an appropriate cartridge and connected to an FPLC Akta Purifier 100 (GE Healthcare, Milan, Italy). The IgG_1 concentration in cell culture supernatant is 0.11 mg/ml, while the investigated flow rates range from 1 to 5 ml/min, corresponding to linear velocities of 29 and 145 cm/h, respectively.

Prior to feeding the complex medium, membranes were preliminarily tested with pure polyclonal IgG solutions under a broad range of different operating conditions. In experiments with pure IgG, 0.1 M phosphate buffered saline (PBS) pH 7.4 was used as loading and washing buffer. Experiments were carried out at four different flow rates, i.e. 1, 2, 5 and 10 ml/min, corresponding to linear velocities of 29, 58, 145 and 290 cm/h, respectively; ten different IgG feed concentrations ranging from 0.14 to 2.15 mg/ml were tested in the chromatographic cycles.

Physical properties of the membranes were obtained with pulse experiments as described in a previous work [25]. The membrane void fraction, ε, is equal to 0.545, while the measured dispersivity coefficient, α, is 0.104 cm. From experiments performed in non adsorbing conditions, the volumes of CSTR and PFR required to describe system dispersion (see Section 4) have been determined as 0.69 and 1.75 ml, respectively [25].

3. Relevant binding mechanisms

Several important information on binding mechanism can be obtained from an accurate study of equilibrium adsorption data derived from experimental breakthrough and washing curves measured under adsorbing and non adsorbing conditions.

The curves shown in Fig. 1 qualitatively represent loading and washing stages, reporting protein concentration in the effluent solution versus the sample volume fed to the column. The different areas identified in this plot have all a precise physical meaning in terms of protein amounts. In particular, the area below the saturation horizontal line and above the breakthrough curve in non adsorbing conditions ($A_{HOLD\ UP}$) represents the amount of protein

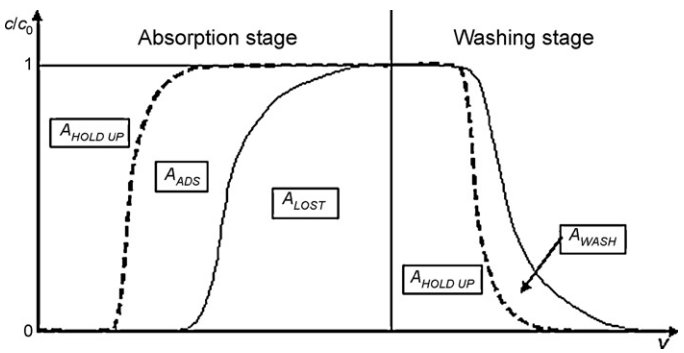

Fig. 1. Qualitative example of the adsorption and washing curves measured under adsorbing (solid line) and non adsorbing (dashed line) conditions. The figure highlights the physical meaning of the different areas in the plot.

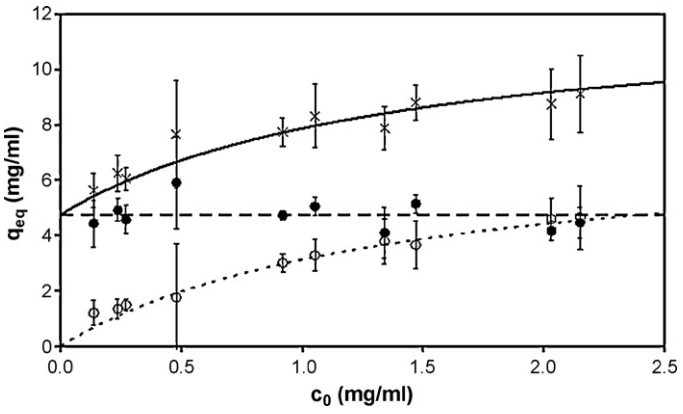

Fig. 2. Equilibrium binding data for total adsorption (×), irreversible contribution (●) and reversible contribution (○). Lines represent the isotherms obtained using the Langmuir model for irreversible (dashed line) and reversible (dotted line) adsorption data and the bi-Langmuir model for total adsorption data (solid line).

which is necessary to fill the hold up volume of the experimental system in the adsorption step; that amount is subsequently removed during washing. The area below the breakthrough curve in adsorbing conditions (A_{LOST}) represents the amount of protein, which is not retained by the column and therefore is lost with effluent solution. Consequently, the area between the two breakthrough curves in adsorbing and non adsorbing conditions (A_{ADS}) is the amount of protein bound onto the affinity column during the adsorption step. Thus, if loading is carried out until column saturation, it is possible to evaluate the overall protein concentration in the solid phase, q_{eq}, in equilibrium with the protein concentration in the mobile phase, c_0. Finally, the area between the washing curves measured under adsorbing and non adsorbing conditions (A_{WASH}) represents the amount of protein that is removed from the affinity column during washing stage. If the washing step is ended when protein concentration in effluent solution reaches the zero baseline, then the amount of protein which is irreversibly adsorbed onto the solid phase can be easily calculated as the difference between the total adsorbed protein in the loading step and the protein desorbed during washing.

By applying the analysis described above, the amounts of protein globally adsorbed in equilibrium with the mobile phase have been calculated, as well as contributions due to reversible and irreversible adsorption. The corresponding results are reported in Fig. 2 in terms of adsorption isotherms.

Isotherm models usually employed to represent protein–ligand adsorption under equilibrium conditions derive from reversible binding kinetics. Indeed, other adsorption mechanisms frequently considered in the literature beyond the commonly used Langmuir model [27] are strictly reversible (e.g. Freundlich, Redlich–Peterson, Toth) [28]. Therefore, consistently with a reversible kinetics, all protein bound in the loading stage should desorb completely from the support during washing, before the protein concentration profile approaches the zero baseline. In contrast, for the experimental system under investigation, as well as in common affinity membrane chromatography, the washing curve reaches the baseline when only a fraction of adsorbed protein is released or desorbed from the stationary phase, indicating that the remaining amount of target protein is bound to the stationary phase in a non reversible manner and cannot be removed from the active sites by using the washing buffer, independently of the duration of the washing step. Indeed, rather long washing steps applied over a one day period have confirmed that conclusion. In addition, equilibrium data for the residual protein amount, which remains adsorbed after washing, do not depend on protein concentration in the mobile phase; thus the corresponding isotherm is practically rectangular as shown in Fig. 2. Coherently with that observation, one has to consider a heterogeneous binding, in which different IgG adsorption sites are present on the membrane surface, each one following a different binding mechanism. For simplicity, in agreement with the results shown in Fig. 2, in this work we consider only two types of independent binding sites, one characterized by a reversible kinetics and the other by an irreversible kinetics.

During washing, protein molecules that interact with the reversible binding sites are completely released in the mobile phase, then the reversible contribution to overall adsorption is characterized also by a weak interaction. Equilibrium adsorption data for both reversible and irreversible binding can be described through a Langmuir isotherm:

$$q_{eq}^{rev} = \frac{c_0 q_m^{rev}}{c_0 + K_d^{rev}}$$
$$q_{eq}^{irr} = \frac{c_0 q_m^{irr}}{c_0 + K_d^{irr}} \quad (1)$$

Since the isotherm associated to irreversible binding is rectangular to all practical purposes (apart at very low c_0 values, where experimental data are not reliable), its dissociation constant is set to zero, so that one has:

$$q_{eq}^{irr} = q_m^{irr} \quad (2)$$

The parameters of the two isotherms, determined through best fitting Eqs. (1) and (2) to equilibrium binding data, are reported in Table 1.

As already reported in previous works, the mimetic ligand B14 is highly specific towards IgG [26,29]. Therefore IgG molecules tend to adsorb strongly onto the available and accessible B14 binding sites of the membrane. On the other hand, modeling analysis conducted previously [25] demonstrated that the main contribution to protein adsorption, represented by specific binding of IgG to the mimetic ligand B14, attains equilibrium conditions almost instantaneously. Consequently, it is rather reasonable to associate specific binding sites to irreversible mechanism and to a very fast kinetics.

On the other hand, weak binding mechanism, related to the reversible reaction, is associated to non specific binding sites and may arise because of different reasons: (i) weak interactions of IgG with the porous matrix, (ii) non directional attachment of B14 ligand on the surface, (iii) ligand moieties immobilized in surface areas that do not allow for a proper formation of B14–IgG complex, (iv) multi-point attachment of protein molecules onto the mimetic ligand and (v) non-homogeneous local peptide density distributions [23,30].

In summary, the strong and irreversible adsorption of IgG molecules onto B14 specific binding sites attains equilibrium conditions instantaneously, while weak reversible IgG adsorption that occurs onto non specific adsorption sites is characterized by a slow binding kinetics.

4. Theoretical model

General features of the mathematical model used in the present work have been presented in a previous paper, where simulation of an affinity membrane chromatography process has been discussed in detail [25]. The mathematical description takes into account the main mass transport phenomena and binding kinetics present in

Table 1
Langmuir parameters of the two adsorption binding sites.

Variable	Irreversible binding	Reversible binding
K_d (mg/ml)	0	1.15
q_m (mg/ml)	4.75	7.00

the membrane column, as well as flow non idealities occurring in all external circuit elements included in the experimental set up, also known as system dispersion.

The overall effects of the external system dispersion are due to a combination of time delay and mixing in the external volumes and they are experimentally characterized by measuring the dynamic response of the system in absence of the membrane module. Such effects can be globally described by using a single PFR and a single CSTR in series, as shown in Refs. [24] and [31]. The same dispersion effects are present also when the membrane module is in place: in such a case, plain conformity to the system configuration would require to consider separately the system elements before and after the membrane module, which cannot be experimentally inspected individually without adding extra volumes. Following well known procedures for non interacting systems in series [32], it is possible to show that it is irrelevant where to locate the membrane module in the series of apparatuses forming the system, as long as the membrane module behaves linearly, since the same transfer function is obtained for all setups. Linearity of column module is followed closely at lower protein saturations, when the solubility isotherm is still linear, while in fact it is no longer valid close to membrane saturation. In order to obtain a good approximation acceptable also for the non linear case, mixing and delay volumes schematized as a sequence of a CSTR and a PFR were considered before the membrane module, since most of the external volumes and flow non-idealities due to pumps and on-line filter are just located prior to the column. Therefore, the analytical solution of the system dispersion model for the adsorption and washing steps considered are:

$$c_{SD} = \begin{cases} 0 & \text{when } t_0^{ads} \le t < t_0^{ads} + t_d \\ c_0 \left[1 - \exp\left(-\frac{F}{V_{CSTR}} (t - (t_d + t_0^{ads})) \right) \right] & \text{when } t_d + t_0^{ads} \le t < t_0^{was} \\ c_0 & \text{when } t_0^{was} \le t < t_0^{was} + t_d \\ c_0 \exp\left(-\frac{F}{V_{CSTR}} (t - (t_d + t_0^{was})) \right) & \text{when } t_d + t_0^{was} \le t \end{cases} \quad (3)$$

where c_{SD} is the protein concentration resulting from the external system dispersion and entering the affinity membrane column, c_0 is the protein concentration in the feed tank, F is the feed flow rate, V_{CSTR} and V_{PFR} are the CSTR and PFR volumes, respectively; t_d is the delay time associated to PFR: $t_d = V_{PFR}/F$; t_0^{ads} and t_0^{was} are the starting times for adsorption and washing stages, respectively [26].

The membrane stack is considered to be a homogenous porous medium of length L, with uniform void fraction ε and uniform maximum binding capacity q_m. The mobile phase flows through the column with constant and uniform interstitial velocity v, since it has been demonstrated that flow distribution at the inlet and flow collection at the outlet are very effective in the membrane module used for experiments [29,33].

The mathematical simulation model includes a species mass balance over the membrane column, coupled with a suitable kinetic equation for the description of interactions between the target molecule and immobilized ligand. In particular, the species mass balance equation accounts for all relevant transport phenomena that are actually present in membrane chromatographic systems, namely convection, axial dispersion and binding/unbinding reactions over the surface. It has been demonstrated that other transport mechanisms such as boundary layer mass transfer, molecular diffusion and surface diffusion are negligible for the stationary media considered. Due to that, they can be completely disregarded in the mathematical description [25,34]. Based on these relevant assumptions, the species mass balance over a membrane column can be expressed as follows:

$$\varepsilon \frac{\partial c}{\partial t} + \varepsilon v \frac{\partial c}{\partial z} = \varepsilon D_L \frac{\partial^2 c}{\partial z^2} - (1 - \varepsilon) \frac{\partial q}{\partial t} \quad (4)$$

where t and z are time and axial coordinate, respectively, v is the interstitial velocity, $D_L = \alpha v$ the longitudinal dispersion coefficient, c and q are the protein concentrations in the mobile phase and stationary phase, respectively.

Adsorption and washing buffers have very similar characteristics in terms of ionic strength, pH and salt content, principally to avoid undesired shocks in affinity column due to buffer change. The main difference between adsorption and washing mixtures is due to the concentration of target protein, which is c_0 during adsorption and is zero during washing. In the present work, the same buffer is used in both adsorption and washing, thus the kinetic equation considered for binding/unbinding is valid for both steps.

More specifically, the kinetic equation used to describe interactions between the target protein and the membrane surface is given by a bi-Langmuir expression, which considers two different binding sites endowed with different binding energies and kinetics. The use of such kinetics is suggested by the experimental evidence discussed in Section 3. The overall protein concentration in the solid phase, q, is obtained by adding contributions of the two different adsorption sites, indicated as q^{irr} and q^{rev} for the irreversible and the reversible binding sites, respectively:

$$q = q^{irr} + q^{rev} \quad (5)$$

Similarly, the overall binding rate results from adsorption/desorption rates of the two different sites:

$$\frac{\partial q}{\partial t} = \frac{\partial q^{irr}}{\partial t} + \frac{\partial q^{rev}}{\partial t} \quad (6)$$

where each kinetic term is represented by a second order equation according to the Langmuir model as follows:

$$\frac{\partial q^i}{\partial t} = k_a^i c \left[(q_m^i - q^i) - K_d^i \frac{q^i}{c} \right] \quad i = irr, rev \quad (7)$$

where k_a^i and K_d^i are the adsorption kinetic rate constant and the Langmuir dissociation constant for the i-th binding sites, respectively.

At the beginning of a chromatographic cycle, protein is not present in the mobile phase nor in the stationary phase. Thus, initial conditions for Eq. (4) can be simply expressed as:

$$c = 0 \quad \text{for} \quad 0 < z < L, \quad t = 0 \quad (8)$$

$$q^{irr} = q^{rev} = 0 \quad \text{for} \quad 0 < z < L, \quad t = 0 \quad (9)$$

Danckwerts boundary conditions for frontal analysis are used to account for axial dispersion at the front surface of the membrane and mixing at the outlet of the membrane module [35]:

$$vc - D_L \frac{\partial c}{\partial z} = v c_{SD} \quad \text{for} \quad z = 0, \quad t > 0 \quad (10)$$

$$\frac{\partial c}{\partial z} = 0 \quad \text{for} \quad z = L, \quad t > 0 \quad (11)$$

The outlet concentration for the system dispersion model represents the actual inlet concentration for the membrane column model [25]. Thus, the right hand side of Eq. (10) is not equal to the protein concentration fed to the system, c_0, but is the value c_{SD}, due to the response of dispersion in the external system.

5. Model results and validation

The numerical value of almost all parameters entering the model, namely the system dispersion parameters, V_{PFR} and V_{CSTR}, as well as membrane properties, ε and α, and thermodynamic constants, K_d^i and q_m^i, are determined through separate and independent experiments. Therefore they are fixed input to the model itself. Only the binding kinetic parameters entering the mathematical description, namely k_a^{irr} and k_a^{rev}, are intrinsically associated to the adsorption process and their value cannot be determined through experiments independent of the chromatographic cycles.

Table 2
Characteristic time scales for the main mass transport steps and reactions involved in the separation process for the experimental system under investigation, at the operating conditions considered.

τ_C (s)	τ_L (s)	τ_a^{irr} (s)	τ_a^{rev} (s)
1.2–12.4	1.2–11.9	$\sim 10^{-5}$	53–810

However, since specific binding interaction between IgG and B14 attains equilibrium conditions instantaneously [25], the kinetic rate constant for specific adsorption is assumed infinitely high and is no longer an adjustable parameter of the model. Vice versa, the reaction rate for the reversible binding reaction, k_a^{rev}, is *a priori* unknown and remains the only adjustable parameter of the presented model. Consistently with its physical meaning, k_a^{rev} must be independent of feed concentration as well as of fluid velocity in the porous medium. Therefore, parameter estimation was obtained by best fitting the model results to the whole experimental data set at all feed flow rates and concentrations. Moreover, since reaction kinetics does not depend on the chromatographic stage considered, the best fitting procedure has been carried out over both adsorption and washing steps, simultaneously. Hence, all simulations use the same numerical value of the fitting parameter k_a^{rev}, for all operating conditions considered and over the entire loading and washing steps.

The model equations proposed to describe the behavior of the membrane stack, Eqs. (4), (6) and (7), constitute a set of PDE, with initial conditions given by Eqs. (8) and (9), and boundary conditions given by Eqs. (10) and (11). The relevant equations, coupled with the algebraic equations, representing the external system dispersion Eq. (3), have been implemented in Aspen Custom Modeler. The numerical value of the kinetic rate constant for very fast irreversible binding, k_a^{irr}, was numerically set to 10^6 ml/(mg min), a value corresponding to infinity to all practical purposes. This assumption is supported by the negligibly low order of magnitude of the corresponding characteristic time for irreversible adsorption (see Table 2), and is also confirmed by the observation that different simulations performed under a range of k_a^{irr} values from 10^2 to 10^6 ml/(mg min) are all superimposed (data not shown). The evaluation of the only fitting parameter considered in this work, k_a^{rev}, has been carried out by using the estimation tool provided with the software and applying the least squares minimization method to the relative concentration error.

5.1. Pure IgG solutions

A preliminary model calibration for estimation of the adjustable parameter k_a^{rev} was carried out by using the experiments conducted with pure IgG solutions. Subsequently, the results obtained were applied to describe the chromatographic cycles using complex mixtures, for which no further adjustable parameters are needed.

Some typical comparisons between experiments measured with pure IgG solutions and simulation results are presented in Fig. 3 for four different operating conditions.

For all operating conditions, the heterogeneous binding model describes well the entire adsorption step, including the broadening behavior close to membrane saturation. In particular, it is apparent that the bi-Langmuir kinetics is able to represent the experimental behavior quite closely, predicting a sharp rise associated to irreversible binding between IgG and the specific B14 adsorption sites, followed by a long tail corresponding to the subsequent saturation of the reversible binding sites. The best fitted value of the kinetic rate constant for reversible adsorption, k_a^{rev}, is equal to 0.53 ± 0.36 ml/(mg min), which corresponds to a characteristic time scale for adsorption, $\tau_a^{rev} = 1/(k_a^{rev} c_0)$, that is always much longer than the characteristic time scale for convection, $\tau_C = L/v$, and longitudinal dispersion, $\tau_L = L^2/D_L$, as summarized in Table 2. Therefore, from the analysis of the relevant characteristic times one realizes that non specific adsorption contribution is kinetically controlled by binding reaction, while specific adsorption is completely controlled by dispersion and convection.

The complete washing step is also accurately described by the model at all operating conditions investigated by using the same

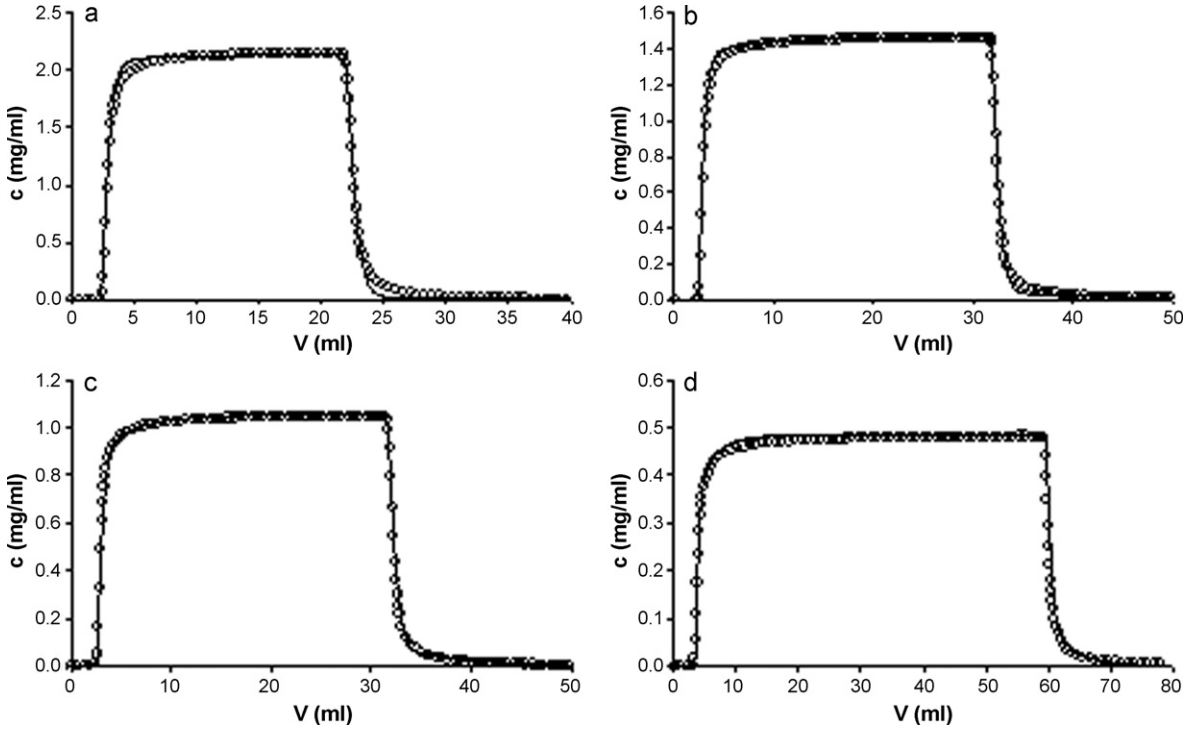

Fig. 3. Comparison between the experimental (○) and simulated (—) breakthrough curves at different operating conditions. (a) v = 290 cm/h, c_0 = 2.15 mg/ml; (b) v = 145 cm/h, c_0 = 1.47 mg/ml; (c) v = 58 cm/h, c_0 = 1.05 mg/ml; (d) v = 29 cm/h, c_0 = 0.48 mg/ml.

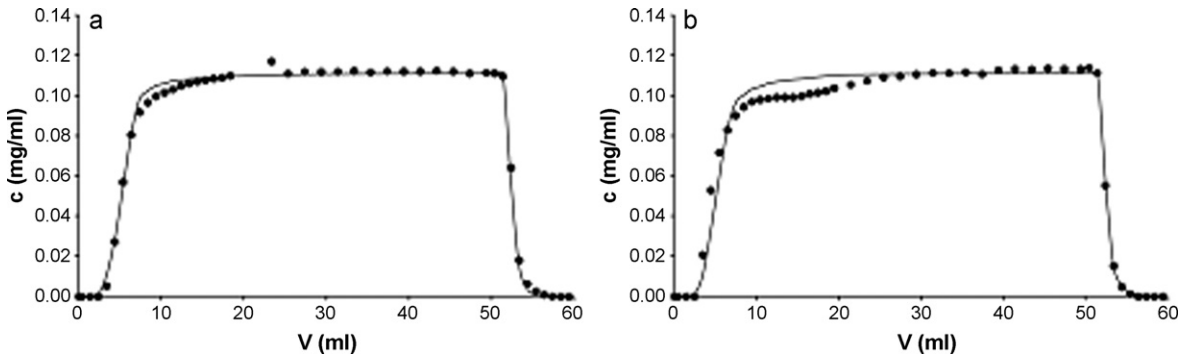

Fig. 4. Comparison between the experimental (●) and simulated (continuous line) loading and washing curves for the IgG species in the runs performed with the complex feedstock at a linear velocity of 145 cm/h (a) and 29 cm/h (b).

value for the adsorption kinetic constant associated to reversible binding sites. The above considerations on the characteristic time scales in the adsorption step are extended to the washing stage: release of non specifically adsorbed IgG molecules from the stationary phase is highly controlled by its binding/unbinding kinetics.

5.2. Cell culture supernatant

In case of experiments performed with cell culture supernatant, the theoretical description of the chromatographic behavior of the membrane support needs also to take into account impurities contained in the feed solution, in addition to IgG. In view of ligand specificity towards IgG, all contaminants present in the supernatant do not interact specifically with the stationary phase investigated and their influence to IgG adsorption can be neglected. As already shown in a previous work [25], their behavior is carefully represented by system dispersion alone and thus the curves for the impurities contained in the feed are not explicitly shown in the present work.

The model parameter obtained for pure IgG feeds is also applied to the case of chromatographic cycles using cell culture supernatant, for which no specific adjustable parameters are needed and the model applies in a completely predictive way to calculate IgG breakthrough curves measured with the complex feed. A comparison between experiments and model prediction is presented in Fig. 4.

The breakthrough curves are highly asymmetrical, with an apparent broadening close to saturation conditions, similarly to what observed in experiments with pure IgG feeds. The model predicts the observed fast concentration growth at the onset of breakthrough and also approximates reasonably well the subsequent tailing behavior; in addition, model description over washing stage is very satisfactory.

The considered bi-Langmuir kinetics is able to describe the entire adsorption and washing profiles simultaneously, thus indicating that the simplified heterogeneous model is fairly accurate for the description of the actual binding mechanism. These observations confirm the reliability of the assumptions made in the mathematical model with particular regard to bi-Langmuir kinetics. Indeed, a simple Langmuir kinetics is unable to represent the tailing behavior present in the experimental breakthrough curves, which can be ascribed to the heterogeneous IgG adsorption on B14-TRZ-Epoxy2 membranes [26].

6. Conclusions

A mathematical model that accurately describes breakthrough broadening close to membrane saturation has been proposed for the simulation of the entire loading and washing steps in membrane affinity chromatography. Detailed equilibrium experiments are required to find appropriate binding kinetics, which is necessary for a proper understanding of protein adsorption on affinity membranes. For the system studied, the residual amount of IgG bound to affinity support after washing is constant, regardless of the experimental feed concentration. That observation is consistent with the existence of a strong irreversible interaction between IgG and the specific B14 moieties. On the other hand, the fraction of IgG, which is released during washing, is due to the presence of weak and reversible binding sites on the membrane surface. Therefore, a heterogeneous binding mechanism has been introduced, and the bi-Langmuir kinetics has been implemented in the mathematical model.

All parameters used in the equations have been properly evaluated through independent measurements, except for the two kinetic rate constants of adsorption, which are intrinsically associated to the adsorption process. The simulation model requires one adjustable parameter, i.e. the kinetic constant for weak and reversible adsorption, since the irreversible binding is infinitely fast.

Model calibration has been carried out by best-fitting experimental adsorption and washing data measured with pure IgG solutions. A good description of the experimental data set has been obtained with the dynamic model proposed, using only one fitting parameter that remains the same over the broad range of operating conditions tested.

In particular, the typical profile of a breakthrough curve appears consistent with the existence of reversible and irreversible binding sites, where the initial concentration growth corresponds to the saturation of the fast and irreversible binding sites and the tailing behavior is due to slow saturation of the reversible adsorption sites.

Model validation has been performed by applying the parameter obtained for pure IgG solutions also for the simulation of the adsorption and washing stages obtained for a cell culture supernatant containing IgG_1. Model simulations are in good agreement with the experimental IgG profile without the need of any further fitting parameter.

This model represents a useful tool for process design and process scale up of membrane affinity chromatography devices and it is likely suitable to predict membrane performance in similar systems. In addition, the interesting separation performances foreseeable for the affinity membranes investigated [26] coupled to the validated model presented in this work represent a convincing input for commercialization of mimetic affinity membranes in the biotechnology market.

Nomenclature

Latin letters

c	protein concentration in the fluid phase, mg/ml
c_0	feed protein concentration in the fluid phase, mg/ml

c_{SD} protein concentration in the fluid phase after system dispersion, mg/ml
q_m maximum binding capacity in the solid phase, mg/ml
q concentration of protein–ligand complex in the solid phase, mg/ml
q_{eq} binding capacity in the solid phase at equilibrium with the concentration in the fluid phase, mg/ml
D_L axial dispersion coefficient, cm^2/s
F flow rate, ml/min
K_d dissociation equilibrium constant, mg/ml
k_a adsorption kinetic rate constant, ml/(mg min)
L total membrane thickness, cm
t time, s
t_0 starting time for the chromatographic stages, s
t_d delay time, s
v interstitial flow velocity, cm/h
V_{PFR} PFR volume in the system dispersion model, ml
V_{CSTR} CSTR volume in the system dispersion model, ml
z axial distance along membrane, cm

Greek letters
α dispersivity coefficient, cm
ε membrane void fraction
τ_L longitudinal dispersion time scale, s
τ_C convection time scale, s
τ_a adsorption time scale, s

Superscripts
ads variable relative to the adsorption step
was variable relative to the washing step
rev variable relative to the reversible reaction
irr variable relative to the irreversible reaction

Acknowledgements

This work has been partly supported by the Sixth Research Framework Programme of the European Union (NMP3-CT-2004-500160), "Advanced Interactive Materials by Design" (AIMs) project, and partly supported by the Italian Ministry of Education and University (MIUR) PRIN 2008 project N. 20085M2L3T, "Development of membrane chromatography for the purification of biomolecules".

References

[1] J.M. Reichert, C.J. Rosensweig, L.B. Faden, M.C. Dewitz, Nat. Biotechnol. 23 (2005) 1073.
[2] A.A. Shukla, B. Hubbard, T. Tressel, S. Guhanb, D. Low, J. Chromatogr. B 848 (2007) 28.
[3] P.A.J. Rosa, A.M. Azevedo, M.R. Aires-Barros, J. Chromatogr. A 1141 (2007) 50.
[4] D. Low, R. O'Leary, N.S. Pujar, J. Chromatogr. B 848 (2007) 48.
[5] B. Kelley, Biotechnol. Progr. 23 (2007) 995.
[6] S. Sommerfeld, J. Strube, Chem. Eng. Process. 44 (2005) 1123.
[7] C. Boi, C. Algeri, G.C. Sarti, Biotechnol. Progr. 24 (2008) 1304.
[8] H. Yang, P.V. Gurgel, R.G. Carbonell, J. Chromatogr. A 1216 (2009) 910.
[9] L. Zamolo, M. Salvalaglio, C. Cavallotti, B. Galarza, C. Sadler, S. Williams, S. Hofer, J. Horak, W. Lindner, J. Phys. Chem. B 114 (2010) 9367.
[10] E. Klein, J. Membr. Sci. 179 (2000) 1.
[11] H. Zou, Q. Luo, D. Zhou, J. Biochem. Biophys. Methods 49 (2001) 199.
[12] R. Ghosh, J. Chromatogr. A 952 (2002) 13.
[13] C. Boi, S. Dimartino, G.C. Sarti, Biotechnol. Progr. 24 (2008) 640.
[14] S.Y. Suen, M.R. Etzel, Chem. Eng. Sci. 47 (1992) 1355.
[15] F.H. Arnold, H.W. Blanch, C.R. Wilke, Chem. Eng. J. 30 (1985) B9.
[16] J.E. Kochan, Y.J. Wu, M.R. Etzel, Ind. Eng. Chem. Res. 35 (1996) 1150.
[17] O.P. Dancette, J.L. Taboureau, E. Tournier, C. Charcosset, P. Blond, J. Chromatogr. B 723 (1999) 61.
[18] K.G. Briefs, M.R. Kula, Chem. Eng. Sci. 47 (1992) 141.
[19] G.C. Serafica, J. Pimbley, G. Belfort, Biotechnol. Bioeng. 43 (1994) 21.
[20] A. Shiosaki, M. Goto, T. Hirose, J. Chromatogr. A 679 (1994) 1.
[21] W. Shi, F. Zhang, G. Zhang, J. Chromatogr. A 1081 (2005) 156.
[22] H. Yang, M.R. Etzel, Ind. Eng. Chem. Res. 42 (2003) 890.
[23] G. Wang, R.G. Carbonell, J. Chromatogr. A 1078 (2005) 98.
[24] C. Boi, S. Dimartino, G.C. Sarti, J. Chromatogr. A 1162 (2007) 24.
[25] S. Dimartino, C. Boi, G.C. Sarti, J. Chromatogr. A 1218 (2011) 1677.
[26] C. Boi, S. Dimartino, S. Hofer, J. Horak, S. Williams, G.C. Sarti, W. Lindner, J. Chromatogr. B 879 (2011) 1633.
[27] I. Langmuir, J. Am. Chem. Soc. 38 (1916) 2221.
[28] S.Y. Suen, J. Chem. Tech. Biotechnol. 65 (1996) 249.
[29] Dimartino, S., Studio sperimentale e modellazione della separazione di proteine con membrane di affinità, Ph.D. Thesis, Università di Bologna, 2009.
[30] E.X. Perez-Almodovar, G. Carta, J. Chromatogr. A 1216 (2009) 8339.
[31] F.T. Sarfert, M.R. Etzel, J. Chromatogr. A 764 (1997) 3.
[32] G. Stephanopoulos, Chemical Process Control: An Introduction to Theory and Practice, Prentice Hall, Engelwood Cliffs, NJ, 1999.
[33] F. Morselli, Graduate Thesis, Università di Bologna, Bologna, 2008.
[34] H.C. Liu, J.R. Fried, AIChE J. 40 (1994) 40.
[35] P.V. Danckwerts, Chem. Eng. Sci. 2 (1953) 1.